Cancer Science
Japanese Cancer Association JCA
Open Access

Tumor miR-125b predicts recurrence and survival of patients with clear-cell renal cell carcinoma after surgical resection

Qiang Fu,[1] Zheng Liu,[1] Deng Pan,[1] Weijuan Zhang,[2] Le Xu,[3] Yu Zhu,[4] Haiou Liu[1] and Jiejie Xu[1]

[1]Key Laboratory of Glycoconjugate Research, MOH, Department of Biochemistry and Molecular Biology, School of Basic Medical Sciences, Shanghai Medical College of Fudan University, Shanghai; [2]Department of Immunology, School of Basic Medical Sciences, Shanghai Medical College of Fudan University, Shanghai; [3]Department of Urology, Zhongshan Hospital, Shanghai Medical College of Fudan University, Shanghai; [4]Department of Urology, Ninth People's Hospital, School of Medicine, Shanghai Jiaotong University, Shanghai, China

Key words

Cancer-specific survival, clear-cell renal cell carcinoma, microRNA-125b, prognostic biomarker, recurrence-free survival

Correspondence

Jiejie Xu, Shanghai Medical College of Fudan University, Mailbox 103, 138 Yixueyuan Road, Shanghai 200032, China.
Tel: +86 21 54237332; Fax: +86 21 64437203;
E-mail: jjxufdu@fudan.edu.cn

Funding information

This work was supported by grants from the National Basic Research Program of China (2012CB822104, 2010CB912104), the National Key Projects for Infectious Diseases of China (2012ZX10002-012), the National Natural Science Foundation of China (31100629, 31270863, 81472227, 81471621, 81402082, 81402085 and J1210041), the Program for New Century Excellent Talents in University (NCET-13-0146) and the Shanghai Rising-Star Program (13QA1400300). All these study sponsors had no role in the study design, or in the collection, analysis and interpretation of data.

Received May 28, 2014; Revised August 7, 2014; Accepted August 19, 2014

Cancer Sci **105** (2014) 1427–1434

doi: 10.1111/cas.12507

The present study aims to evaluate the impact of tumor microRNA-125b (miR-125b) on recurrence and survival of patients with clear-cell renal cell carcinoma (ccRCC) following surgery. We retrospectively enrolled 276 patients (200 in the training cohort and 76 in the validation cohort) with ccRCC undergoing nephrectomy at a single institution. Clinicopathologic features, cancer-specific survival (CSS) and recurrence-free survival (RFS) were recorded. Tumor miR-125b levels were assessed by *in situ* hybridization (ISH) in specimens of patients. The Kaplan–Meier method was applied to compare survival curves. Cox regression models were used to analyze the impact of prognostic factors on CSS and RFS. A concordance index (C-index) was calculated to assess predictive accuracy. In both cohorts, tumor miR-125b positively correlated with Fuhrman grade. High tumor miR-125b indicated poor survival and early recurrence for patients with ccRCC, especially with advanced stage disease. After multivariable adjustment, tumor miR-125b was identified as an independent adverse prognostic factor for survival and recurrence. The predictive accuracy of traditional TNM and UCLA Integrated Staging System prognostic models was improved when tumor miR-125b was added. The results showed that tumor miR-125b is a potential independent adverse prognostic biomarker for recurrence and survival of patients with ccRCC after nephrectomy.

Renal cell carcinoma (RCC) is the major malignancy derived from renal tubular epithelial cells, and represents a spectrum of histologic subtypes.[1] The main one, accounting for nearly 80% of RCC and with an incidence rate of 17.8 in Europe and 20.6 in USA per 100 000 individuals in 2013, is clear-cell RCC (ccRCC).[2,3] ccRCC is associated with high metastasis risk and some degree of chemotherapy resistance. The estimated 5-year mortality rate of patients undergoing resection is 15–30%, accompanied by a recurrence rate as high as 20–40%.[4] Considering the poor and fickle prognosis, outcome prediction for ccRCC has been an important research subject.[5] However, the current distinction relies on morphology and pathology is not conclusive for all ccRCC patients, probably because of their complicated cytogenetical features,[5,6] which propels us to explore the feasibility of applying other prognostic factors, such as genomic alterations, proteomic analysis, immunotransmitter or microRNA.[7]

MicroRNA (miRNA) are a class of 19–25 nucleotide noncoding RNA molecules that could induce post-transcriptional silencing of target genes by interacting with their 3′-UTR, thus regulating many important biological processes such as cell development, differentiation and apoptosis.[8] Dysregulation of miRNA and relevant complex mechanisms have been observed in ccRCC cases.[9] It is notable that many cancer-dysregulated miRNA show dynamic expression and their targets may alter depending on practical circumstances.[10] For example, miR-34a is overexpressed in ccRCC and accelerates proliferation, whereas it is downregulated and targets oncogene *CDK6* in other urologic neoplasms.[8]

In view of the important regulatory roles miRNA play in cancer development and progression, many studies have been carried out to identify miRNA as potential biomarkers for ccRCC diagnosis, prognosis and personalized therapy.[6,11–13] Saini *et al.*[14] report that miR-708 induced apoptosis and suppressed tumorigenicity in RCC. In addition, a profile of

miR-21/141/155 was proposed by Silva-Santos *et al.*,[15] which was expected to convey further prognostic information. We noticed that previous studies had discovered increased expression of miR-125b in advanced metastatic ccRCC compared to primary/none metastatic tumors, yet the exact role it plays in ccRCC remains undefined. This phenomenon prompted us to assess whether it is a potential biomarker.[11,16]

For this study, we evaluate the expression of miR-125b in 276 formalin-fixed paraffin-embedded (FFPE) ccRCC specimens by *in situ* hybridization (ISH), and analyze the relationship between its expression and clinicopathologic characteristics or clinical outcome, including cancer-specific survival (CSS) and recurrence-free survival (RFS). We further assess prognostic values of miR-125b expression and evaluate its ancillary efficiency when added to well-established predictive models.

Materials and Methods

Patients and database. In this retrospective study, we used 397 FFPE tissue samples collected from Zhongshan Hospital (Shanghai, China). The study was approved by Zhongshan Hospital's ethics committee and informed consent was obtained from each participant. All patients involved underwent surgical nephrectomy and had not been previously treated with chemotherapy or radiotherapy. We excluded the patients that had no FFPE tumor sample, that presented other subtypes of tumor besides ccRCC, and those without available follow-up information. Patients who did not survive for more than 1 month were considered to have died of postoperative complications and were excluded from the study. Sections that easily fell off during standard ISH procedure were also excluded.

We assigned 200 patients from between 2 January 2003 and 30 December 2004 to the training set, and 76 patients from between 1 January 2001 and 31 December 2001 to the validation set. All concomitant data, including age, gender, Fuhrman grade, tumor size, coagulative necrosis, TNM and Eastern cooperative Oncology Group performance status (ECOG-PS), were obtained from the hospital's pathologic records, and reassessed by two pathologists (L. Chen and H. Fu) intensively using H&E-stained paraffin sections.

We macrodissected and discarded areas of necrosis, hemorrhagic, fibrosis or any kind of regressive degeneration before building tissue microarrays (TMA). To construct TMA, we chose two representative and homogeneous cores with 1.0-mm diameter from different positions for each tumor. The TMA samples comprised more than 80% tumor cells. TNM stage was classified according to 2010 American Joint Committee on Cancer TNM classification.[17] UCLA Integrated Staging System (UISS) and Mayo clinic stage, size, grade and necrosis (SSIGN) were recorded as previously described.[18,19] CSS was defined as the time from the date of surgery to the date of ccRCC-relevant death, and RFS as the time from surgery to confirmed tumor relapse. Cases were censored at the date of death from other causes, or the date of last follow-up visit. We defined metastasis cases as any N1 or M1 stage tumor, and did not include them as RFS. Patients with localized RCC ($n = 259$) were treated with radical or partial nephrectomy while metastatic patients ($n = 17$) were treated with cytoreductive nephrectomy. The median survival times of CSS were 88.15 (9–120) for the training set and 72.12 (18–119) for the validation set. Median RFS were 82.87 (7–120) for the training set and 62.44 (17–114) for the validation set.

***In situ* hybridization analysis.** The ISH procedure was carried out with miR-125b miRCURY LNA microRNA Detection Probes (Exiqon, Woburn, MA, USA) and a miRCURY LNA microRNA ISH Optimization Kit (FFPE) (Exiqon). The 5′-3′ sequences of probes were TCACAAGTTAGGGTCTCAGGGA, with both 5′ and 3′ ends DIG labeled. The ISH procedure was optimized according to the instruction manual to achieve satisfactory results: a 37°C 15-min incubation of 1 μL/mL proteinase-K, a 56°C 3-h hybridization of 40-nM miR-125b probes and a 4°C 9-h incubation of 1:400 anti-DIG-AP (Roche, Basel, Switzerland) were applied.

Two urologic pathologists (L. Chen and H. Fu) reviewed the staining sections and for every sample, each of them chose a typical field under 10 × 20 magnification independently, without knowing any information about the patients. The score of tumor cores was determined by their deliberation if their two scores were different. Then the arithmetic average of the two scores from the same tumor is determined as a quantification of tumorous miR-125b. A semi-quantitative evaluation was then used: percentages of miR-125b-positive cells were scored from 0 to 100, intensities of staining were scored from 0 to 3 (from low to high, respectively), and the products of percentage × intensity were recorded; the mean point by two pathologists was determined as the final score of that sample.

Statistical analysis. Using the X-tile program (version 3.6.1; Yale, New Haven, USA), a cutoff point for a continuous variable according to the highest χ^2 of Kaplan–Meier analysis was selected. Using SPSS (version 21.0; IBM, Armonk, NY, USA), Student's *t*-test, the χ^2-test or Fisher's exact test were used to compare variables between two groups. Univariate and multivariate Cox proportional hazards regression were used to carry out analysis of the association between miR-125b expression and clinicopathological features or survival. Hazard ratios (HR) with 95% CI were calculated for each factor or variable level. Using MedCalc (version 12.7; Mariakerke, Belgium), the Kaplan–Meier method was applied to plot the survival curves, and results of log-rank test were added. Using Stata (version 12.1; StataCorp LP, TX, USA), Harrell's concordance index (C-index) and Akaike's information criterion (AIC) were generated to compare the predictive ability of various models with or without the addition of miR-125b. Bootstraps with 1000 resamples were used for Cox regression, C-index and AIC assessments. All tests were two-sided and a level of $P < 0.05$ was considered statistically significant.

Results

***In situ* hybridization findings and correlation analysis with clinicopathologic features.** To identify clinical significance of miR-125b expression in ccRCC progression, we carried out ISH of miR-125b with ccRCC samples chosen with the criteria described above; 276 samples had successful staining. In 260 (94.20%) specimens, specific miR-125b expression outside the nucleus was observed (Fig. S1) and showed varying staining intensity.

According to a score of 17.5 selected by the X-tile program based on the training set as a global cutoff point, 112 of 200 cases in the training set and 44 of 76 in the validation set were categorized as belonging to the low group; the remaining 88 of 200 and 32 of 76 cases were categorized as belonging to the high group, respectively. We further looked into the correlations between miR-125b and clinical pathologic features and found that increased miR-125b expression was correlated with high Fuhrman grade in the two independent sets ($P < 0.001$ and $P = 0.004$, respectively; Table S1). These findings indicated that miR-125b expression was elevated in ccRCC tissues with poorer histological differentiation.

Associations between miR-125b expression and cancer-specific survival or recurrence-free survival in patients with clear-cell renal carcinoma. To establish whether miR-125b expression was associated with the outcome of ccRCC patients, we compared the CSS between miR-125b high and low expression subgroups by Kaplan–Meier analysis and log-rank test. The result showed that patients with high miR-125b expression had a poorer survival rate ($P = 0.007$) than those with low expression in the training set. When stratified by TNM stage, miR-125b expression showed significantly prognostic value for TNM III + IV advanced stage tumors ($P < 0.001$) with respect to TNM I + II early stage tumors in the training set ($P = 0.131$) (Fig. 1a). Similar results in the validation set ($P = 0.001$, 0.032 and 0.086, respectively; Fig. 1b) were observed. To specially identify the prognostic significance, univariate Cox analysis of miR-125b expression was conducted in the entire cohort of 276 cases (HR 1.986, 95% CI 1.102–3.758, $P = 0.024$), in all 80 advanced stage cases (HR 6.787, 95% CI 3.013–29.459, $P = 0.001$) and in all 196 early stage cases (HR 1.008, 95% CI 0.418–2.411, $P = 0.987$) (Fig. 1c).

Moreover, we excluded all metastasis cases with any N1 or M1 stage tumors because of their substantial correlation with recurrence, and investigated the association between miR-125b expression and RFS after that. Patients with high miR-125b expression had shorter RFS than those with low expression in the training set ($P = 0.002$) and the validation set ($P < 0.001$); the prognostic significance remained in stratified T2–4 classification patients of two independent sets ($P < 0.001$ and $P = 0.018$, respectively) (Fig. 2a,b). The Cox analysis results of miR-125b in different subgroups are shown in Figure 2(c): high miR-125b expression was connected with high risk of recurrence in all 259 cases (HR 2.396, 95% CI 1.365–4.778, $P = 0.005$) and 96 cases of T2–4 patients (HR 6.366, 95% CI 2.754–25.508, $P = 0.001$), but did not in 173 cases of T1 patients (HR 1.507, 95% CI 0.614–3.857, $P = 0.363$).

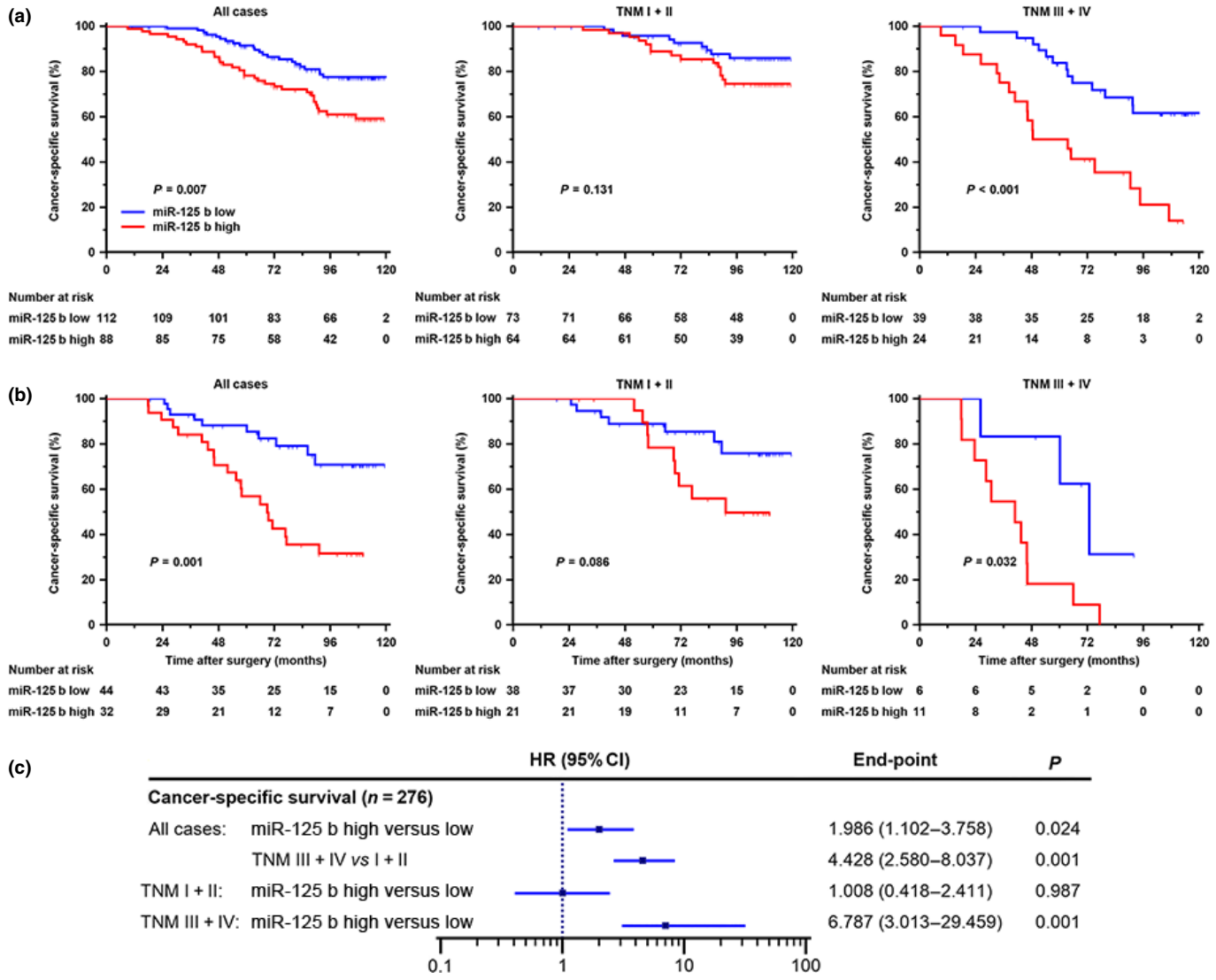

Fig. 1. Kaplan–Meier analysis of cancer-specific survival (CSS) for patients with clear-cell renal carcinoma (ccRCC) in the training and validation sets, and univariate Cox analysis for the predictive value of miR-125b in the overall patients. (a) Kaplan–Meier analysis of CSS for different ccRCC patient subgroups in the training set, $n = 200$. (b) Kaplan–Meier analysis of CSS for different ccRCC patients subgroups in the validation set, $n = 76$. (c) Univariate Cox analysis of miR-125b expression on CSS for different subgroups, in all cases, $n = 276$. *P*-value was calculated by log-rank test.

Taken together, these results indicate that miR-125b expression correlates with CSS and RFS for patients with ccRCC, especially for the advanced stage.

High miR-125b expression is an independent predictor of poor prognosis for with clear-cell renal cell carcinoma patients. We proceed with univariate and multivariate analysis for CSS and RFS in the training set to verify whether miR-125b is an independent predictor. Age, gender, coagulative necrosis, size, ECOG-PS, Fuhrman grade, TNM stage or T stage, and miR-125b expression were included in the univariate analysis: the variables identified as risk factors were further involved in the multivariate analysis. After multivariable adjustment by clinicopathological variables, ECOG-PS (P = 0.023), Fuhrman grade (P = 0.037), TNM stage (P = 0.003) and miR-125b expression in particular (HR 2.316, 95% CI 1.263–4.244, P = 0.011) were identified as independent prognostic factors for CSS, while Fuhrman grade (P = 0.007), T stage (P = 0.001) and miR-125b expression in particular (HR 1.860, 95%CI 1.059–3.269, P = 0.030) as independent prognostic factors for RFS (Tables 1 and 2).

We also performed the same procedure for the validation set. Coagulative necrosis was kept to multivariate analysis to possess comparability between two cohorts,though it was not significant for CSS(HR 1.487, 95% CI 0.679–3.258, P = 0.321) in univariate analysis of the validation set. The adjusted results mirrored those for the training set (Tables 1 and 2), which indicated that high miR-125b expression was an independent predictor of poor prognosis for ccRCC patients.

Extension of established prognostic models with miR-125b expression. We added miR-125b expression as a binary variable to well-established prognostic systems (TNM stage, UISS and SSIGN) to see if it could improve the prognostic power of these systems. All cases of the two independent sets were included. As shown in Table 3, for the endpoint of CSS, the addition of miR-125b expression with TNM stage (C-index 0.715, 95% CI 0.656–0.773) or UISS (C-index 0.719, 95% CI

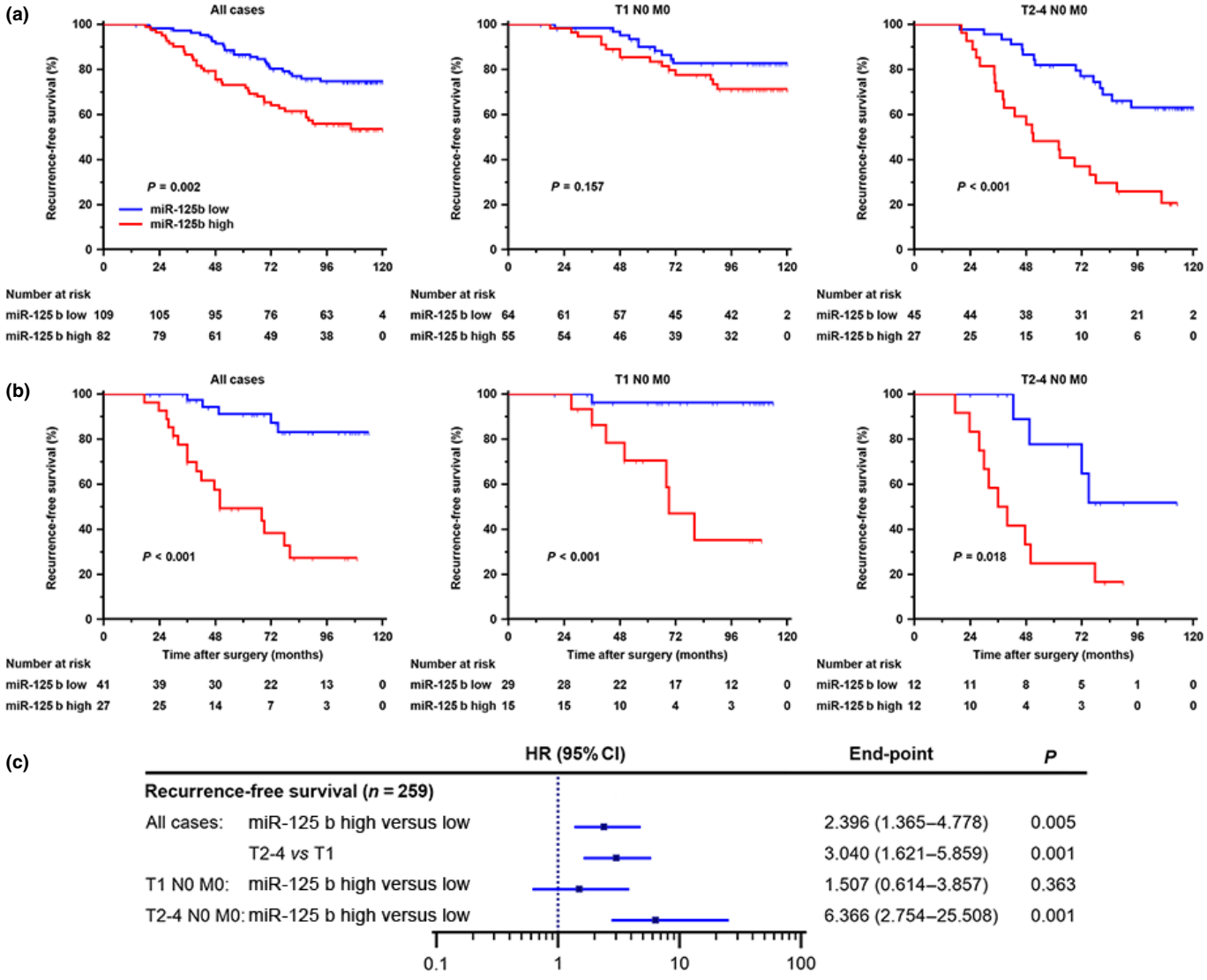

Fig. 2. Kaplan–Meier analysis of recurrence-free survival (RFS) for patients with clear-cell renal carcinoma (ccRCC) in the training and validation sets, and univariate Cox analysis for the predictive value of miR-125b in the overall patients. (a) Kaplan–Meier analysis of RFS for different ccRCC patients subgroups in the training set, n = 191. (b) Kaplan–Meier analysis of RFS for different ccRCC patients subgroups in the validation set, n = 68. (c) Univariate Cox analysis of miR-125b expression on RFS for different subgroups, in all cases, n = 259. P-value was calculated by log-rank test.

Table 1. Univariate and multivariate Cox regression analyses for cancer-specific survival in the training and validation sets

Variable	Training set				Validation set			
	Univariate analysis		Multivariate analysis		Univariate analysis		Multivariate analysis	
	HR (95% CI)	*P*	HR (95% CI)	*P*	HR (95% CI)	*P*	HR (95% CI)	*P*
Age (≥60 *vs* <60)	1.642 (0.958–2.883)	0.065	–	NA	1.775 (0.914–3.920)	0.114	–	NA
Gender (Male *vs* Female)	0.988 (0.589–1.822)	0.978	–	NA	1.289 (0.593–3.494)	0.556	–	NA
Coagulative necrosis (yes *vs* no)	2.815 (1.550–4.933)	0.001	1.596 (0.866–2.941)	0.165	1.487 (0.679–3.258)	0.321	0.572 (0.232–1.410)	0.225
Tumor size (≤4 cm *vs* >4 cm)	1.822 (1.042–3.187)	0.027	0.719 (0.377–1.372)	0.327	1.990 (1.010–4.393)	0.048	0.851 (0.330–2.195)	0.738
ECOG-PS (≥1 *vs* 0)	3.080 (1.742–5.479)	0.001	2.212 (1.201–4.072)	0.023	5.675 (2.732–14.895)	0.001	5.825 (1.775–19.116)	0.004
Fuhrman grade		<0.001		0.037		<0.001		0.049
2 *vs* 1	1.802 (0.663–11.123)	0.258	1.249 (0.355–4.392)	0.684	1.410 (0.382–5.213)	0.606	2.009 (0.465–8.672)	0.350
3 *vs* 1	2.892 (1.116–16.544)	0.031	2.465 (0.702–8.661)	0.119	6.701 (1.782–25.197)	0.005	7.411 (1.432–38.343)	0.017
4 *vs* 1	8.574 (2.808–26.183)	0.001	3.173 (0.807–12.478)	0.066	6.298 (1.695–23.404)	0.006	4.738 (0.937–23.967)	0.060
TNM-stage (III + IV *vs* I + II)	3.888 (2.275–6.753)	0.001	3.378 (1.737–6.571)	0.003	6.385 (3.071–17.779)	0.001	6.672 (2.724–16.343)	0.001
miR-125b (high *vs* low)	2.068 (1.178–3.644)	0.009	2.316 (1.263–4.244)	0.011	3.333 (1.709–8.356)	0.004	3.005 (1.059–8.525)	0.039

HR, Hazard Ratio; 95%CI, 95% confidence interval; ECOG-PS, Eastern cooperative Oncology Group performance status; NA, not adopted. All HR and 95%CI are calculated from 1000 bootstrap samples to protect from overfitting.

Table 2. Univariate and multivariate Cox regression analyses for recurrence-free survival in the training and validation sets

Variable	Training set				Validation set			
	Univariate analysis		Multivariate analysis		Univariate analysis		Multivariate analysis	
	HR (95% CI)	*P*	HR (95% CI)	*P*	HR (95% CI)	*P*	HR (95% CI)	*P*
Age (≥60 *vs* <60)	1.586 (0.971–2.570)	0.056	–	NA	0.677 (0.308–1.359)	0.298	–	NA
Gender (Male *vs* Female)	1.015 (0.618–1.793)	0.955	–	NA	0.680 (0.322–1.502)	0.293	–	NA
Coagulative necrosis (yes *vs* no)	2.507 (1.556–4.166)	0.001	1.187 (0.649–2.168)	0.578	2.978 (1.253–7.078)	0.014	1.675 (0.581–4.827)	0.340
Tumor size (≤4 cm *vs* >4 cm)	1.974 (1.219–3.323)	0.004	0.906 (0.500–1.643)	0.746	2.664 (1.343–6.309)	0.006	0.546 (0.102–2.929)	0.480
ECOG-PS (≥1 *vs* 0)	2.821 (1.699–4.623)	0.001	1.771 (0.965–3.253)	0.065	4.391 (1.935–11.635)	0.001	0.851 (0.167–4.338)	0.846
Fuhrman grade		<0.001		0.007		<0.001		0.003
2 *vs* 1	2.125 (0.732–6.166)	0.166	1.417 (0.476–4.220)	0.532	3.635 (0.454–29.126)	0.224	1.154 (0.117–11.379)	0.902
3 *vs* 1	3.816 (1.314–11.076)	0.014	2.968 (0.989–8.902)	0.052	15.672 (1.813–135.474)	0.012	1.775 (0.127–24.782)	0.670
4 *vs* 1	9.989 (3.245–30.749)	0.001	4.122 (1.222–13.905)	0.022	86.055 (9.098–813.966)	0.001	13.536 (1.085–168.860)	0.043
T-stage (T2-4 vs T1)	2.886 (1.765–5.048)	0.001	2.923 (1.566–5.459)	0.001	4.179 (1.872–11.681)	0.001	5.600 (1.126–27.848)	0.035
miR-125b (high *vs* low)	2.162 (1.331–3.662)	0.003	1.860 (1.059–3.269)	0.030	4.328 (1.820–12.354)	0.001	3.931 (1.213–12.740)	0.022

HR, Hazard Ratio; 95%CI, 95% confidence interval; ECOG-PS, Eastern cooperative Oncology Group performance status; NA, not adopted. All HR and 95%CI are calculated from 1000 bootstrap samples to protect from overfitting.

0.661–0.777) showed markedly higher prognostic accuracy than the original TNM stage (C-index 0.664, 95% CI 0.614–0.715) or original UISS (C-index 0.687, 95% CI 0.632–0.742), but it did not when combined with SSIGN (C-index 0.725, 95% CI 0.666–0.783) compared with the original SSIGN (C-index 0.716, 95% CI 0.656–0.776). We observed a similar result for RFS. We also calculated the AIC for each model; with a lower AIC score, the combination of miR-125b and TNM stage or UISS still exhibited greater prognostic power than TNM stage or UISS alone for CSS, as well as RFS (Table 3).

Discussion

Here, our findings show that, in ccRCC cases, high expression of miR-125b was significantly correlated with poor histological differentiation. The results of multivariate and Kaplan–Meier analyses indicated miR-125b to be an independent prognostic factor of poor CSS and RFS, especially for the advanced tumors. Combinations of miR-125b signature and TNM stage or UISS could further stratify patients and provide higher prognostic power.

In routine clinical practice, TNM stage is the key prognostic determinant for ccRCC patients.[20,21] However, it is reported that some of the substages identified by TNM stage show overlapping prognoses, while other substages contain patients with heterogeneous outcomes.[22,23] This also occurs with other extended anatomy-based models like UISS and SSIGN.[24,25] There has been rapid improvement in the understanding of the molecular biology of ccRCC and various biomarkers associated with prognosis have been reported, such as C-reactive protein,[26] providing different prognostic information. miRNA have drawn ever greater attentions. For instance, as a consequence of Von Hippel-Lindau (VHL) gene inactivating mutation, HIF-1/2 contributed to overexpression of miR-210, which reduced reactive oxygen species production through targeting iron sulphur cluster homologue (ISUC), and correlates with favourable clinicopathological factors.[27] Hence, it may be a simple and easy-to-use clinical procedure to identify miRNA in ccRCC with quantitative or semi-quantitative assays.

Table 3. Comparison of the prognostic accuracies of miR-125b expression, TNM-stage, UISS and SSIGN scoring system in all cases

	C-index (95%CI)	AIC
Cancer-specific survival (n = 276)		
miR-125b	0.611 (0.558–0.664)	890.64
TNM	0.664 (0.614–0.715)	868.86
TNM + miR-125b	0.715 (0.656–0.773)	846.88
UISS	0.687 (0.632–0.742)	842.68
UISS + miR-125b	0.719 (0.661–0.777)	834.03
SSIGN	0.716 (0.656–0.776)	845.21
SSIGN + miR-125b	0.725 (0.666–0.783)	841.35
Recurrence-free survival (n = 259)		
miR-125b	0.623 (0.571–0.676)	857.83
TNM	0.626 (0.574–0.678)	850.61
TNM + miR-125b	0.697 (0.641–0.752)	826.33
UISS	0.653 (0.608–0.699)	842.27
UISS + miR-125b	0.705 (0.654–0.756)	831.24
SIGN	0.711 (0.656–0.766)	828.10
SSIGN + miR-125b	0.723 (0.667–0.780)	821.99

C-index, concordance index; 95%CI, 95% confidence interval; AIC, Akaike's information criterion; UISS, UCLA Integrated Staging System; SSIGN, Mayo clinic stage, size, grade, and necrosis. C-index, 95%CI and AIC are calculated from 1000 bootstrap samples to protect from overfitting.

It is well-known that miR-125b plays a crucial role in cell growth, apoptosis and metastasis. In bladder cancer, miR-125b suppressed the development of tumor by targeting E2F3, a transcription factor that induced cells to transit from G1 to S cell cycle phase.[28] In prostate cancer, miR-125b promoted xenograft tumor growth, probably through directly targeting three key pro-apoptosis genes: *P53*, *PUMA* and *BAK1*.[29] This ectopic expression of miR-125b has also been seen in ovary, breast, liver, leukemia and glioma cancer. Depending on the different tissular and cellular context, respective genes were targeted by miR-125b, revealing its multi-face character as an oncogene or a tumor suppressor.[30–34] Accordingly, it is valuable to apply miR-125b in cancer diagnosis and prognosis as a supplement of clinic classification approaches. Nishida *et al.* demonstrate that high expression levels of miR-125b are associated with enhanced malignant potential in colorectal cancer, and could be an independent predictor of poor prognosis for patients who have undergone complete colorectum resection.[35]

However, studies on the role of miR-125b in ccRCC are limited and the underlying mechanisms remain largely unknown. It has been revealed that miR-125b is expressed at low levels in normal renal tubular epithelial cells and interstitial cells,[36] and is expressed higher in advanced metastatic ccRCC than primary/non-metastatic ccRCC.[16] Consistent with these results, we showed high miR-125b expression in aggressive tumors; those patients with advanced stage and high expression of miR-125b had shorter CSS and RFS. The present study highlights the possibility that miR-125b may be directly involved in the metastatic process of ccRCC. Interestingly, miR-125b was found to target erythropoietin and its receptor, correlating with metastatic potential in breast cancer.[37] Through a series of *in vivo* experiments on nude mice, Wan *et al.* found that miR-125b was significantly higher in SU3 cells, a highly invasive and progenitor glioma stem cell line. This oncogene-like behavior probably follow the inhibition of a novel target gene of miR-125b, matrix metalloprotease 9.[38]

Our findings may be used to improve the predictive ability of some well-established models, such as TNM stage and UISS. The possibility of using the expression of microRNA as prognostic biomarkers or molecular classifiers has been investigated in several cancer types, including RCC. For example, Brandenstein *et al.* found that miR-15a, together with its upstream PKCα, could differentiate benign and malignant renal tumors in fresh biopsy samples.[39] In addition, Fritz *et al.*[40] reveal that the ratio of miR-21/10b expression significantly correlates with disease severity and survival of non-metastasis ccRCC. Although nowadays RCC can often be diagnosed fairly certainly without a biopsy, and CT/MRI scans can be helpful in diagnosing most kinds of kidney tumors, miR-125b staining on biopsy specimens could be mainly used as a biomarker in prognostic stratification and molecular classification of RCC after nephrectomy, based on the maturity of renal resection operation and detectability of miR-125b, as we showed in this study.

Novel therapies are perhaps the most exciting aspect in the study of miRNA in cancers. miR-125b have been found to target several tumor suppressor genes in different human malignancies. Haemmig *et al.*[41] found that in glioblastomas miR-125b targeted TNFAIP3/NKIRAS2, relieved the inhibitory of NF-κB and, therefore, controls apoptosis as well as

temozolomide resistance. Gurova *et al.*[42] proved the activation of NF-κB signaling pathway in RCC, indicating the possibility of delivering synthetic miR-125b inhibitor into patients to suppress the tumorous functions of NF-κB. In view of the important roles NF-κB signaling plays in molecularly-targeted therapy with sorafenib, and the finding that IFN-α, another first-line therapy agent of ccRCC, could downregulate miR-125b in monocyte differentiation,[43] it might be possible to enhance the chemotherapy effect through a combination of cytokine and targeted therapy drugs. Besides, octamer-binding transcription factor 4 (OCT4) induces upregulation of miR-125b through directly binding to the promoter of miR-125b in cervical lesions, which could probably be reversed under high doses of docetaxel treatment.[44,45]

However, this work has limitations in terms of generalizability because all cases were obtained from a single institution in China, and it is necessary to acquire independents datasets from non-Asian patients to confirm the prognostic value of miR-125b in ccRCC. Last, but equally important, further investigation into miR-125b's functions and additional targets should be conducted so as to provide more information for better understanding of the detailed molecular mechanisms.

Acknowledgments

We thank Ms Haiying Zeng (Department of Pathology, Zhongshan Hospital, Shanghai Medical College of Fudan University) for technical assistance.

Disclosure Statement

This work was supported by grants from the National Basic Research Program of China (2012CB822104, 2010CB912104), the National Key Projects for Infectious Diseases of China (2012ZX10002-012), the National Natural Science Foundation of China (31100629, 31270863, 81472227, 81471621, 81402082, 81402085 and J1210041), the Program for New Century Excellent Talents in University (NCET-13-0146) and the Shanghai Rising-Star Program (13QA1400300). These study sponsors had no role in the study design or in the collection, analysis and interpretation of data and, hence, the authors have no conflict of interest to declare.

References

1 Nelson EC, Evans CP, Lara PN Jr. Renal cell carcinoma: current status and emerging therapies. *Cancer Treat Rev* 2007; **33**: 299–313.
2 Wach S, Nolte E, Theil A *et al.* MicroRNA profiles classify papillary renal cell carcinoma subtypes. *Br J Cancer* 2013; **109**: 714–22.
3 Siegel R, Naishadham D, Jemal A. Cancer statistics, 2013. *CA Cancer J Clin* 2013; **63**: 11–30.
4 Ljungberg B, Hanbury DC, Kuczyk MA *et al.* Renal cell carcinoma guideline. *Eur Urol* 2007; **51**: 1502–10.
5 Delahunt B, Cheville JC, Martignoni G *et al.* The International Society of Urological Pathology (ISUP) grading system for renal cell carcinoma and other prognostic parameters. *Am J Surg Pathol* 2013; **37**: 1490–504.
6 Wu X, Weng L, Li X *et al.* Identification of a 4-microRNA signature for clear cell renal cell carcinoma metastasis and prognosis. *PLoS ONE* 2012; **7**: e35661.
7 Cancer Genome Atlas Research N. Comprehensive molecular characterization of clear cell renal cell carcinoma. *Nature* 2013; **499**: 43–9.
8 Catto JW, Alcaraz A, Bjartell AS *et al.* MicroRNA in prostate, bladder, and kidney cancer: a systematic review. *Eur Urol* 2011; **59**: 671–81.
9 White NM, Bao TT, Grigull J *et al.* miRNA profiling for clear cell renal cell carcinoma: biomarker discovery and identification of potential controls and consequences of miRNA dysregulation. *J Urol* 2011; **186**: 1077–83.
10 Lu J, Getz G, Miska EA *et al.* MicroRNA expression profiles classify human cancers. *Nature* 2005; **435**: 834–8.
11 Heinzelmann J, Unrein A, Wickmann U *et al.* MicroRNAs with prognostic potential for metastasis in clear cell renal cell carcinoma: a comparison of primary tumors and distant metastases. *Ann Surg Oncol* 2013; **21**: 1046–54.
12 Vergho D, Kneitz S, Rosenwald A *et al.* Combination of expression levels of miR-21 and miR-126 is associated with cancer-specific survival in clear-cell renal cell carcinoma. *BMC Cancer* 2014; **14**: 25.
13 White NM, Yousef GM. MicroRNAs: exploring a new dimension in the pathogenesis of kidney cancer. *BMC Med* 2010; **8**: 65.
14 Saini S, Yamamura S, Majid S *et al.* MicroRNA-708 induces apoptosis and suppresses tumorigenicity in renal cancer cells. *Cancer Res* 2011; **71**: 6208–19.
15 Silva-Santos RM, Costa-Pinheiro P, Luis A *et al.* MicroRNA profile: a promising ancillary tool for accurate renal cell tumour diagnosis. *Br J Cancer* 2013; **109**: 2646–53.
16 Heinzelmann J, Henning B, Sanjmyatav J *et al.* Specific miRNA signatures are associated with metastasis and poor prognosis in clear cell renal cell carcinoma. *World J Urol* 2011; **29**: 367–73.
17 Edge SB, Compton CC. The American Joint Committee on Cancer: the 7th edition of the AJCC cancer staging manual and the future of TNM. *Ann Surg Oncol* 2010; **17**: 1471–4.
18 Zisman A, Pantuck AJ, Wieder J *et al.* Risk group assessment and clinical outcome algorithm to predict the natural history of patients with surgically resected renal cell carcinoma. *J Clin Oncol* 2002; **20**: 4559–66.
19 Frank I, Blute ML, Cheville JC, Lohse CM, Weaver AL, Zincke H. An outcome prediction model for patients with clear cell renal cell carcinoma treated with radical nephrectomy based on tumor stage, size, grade and necrosis: the SSIGN score. *J Urol* 2002; **168**: 2395–400.
20 Kim SP, Alt AL, Weight CJ *et al.* Independent validation of the 2010 American Joint Committee on Cancer TNM classification for renal cell carcinoma: results from a large, single institution cohort. *J Urol* 2011; **185**: 2035–9.
21 Ficarra V, Galfano A, Mancini M, Martignoni G, Artibani W. TNM staging system for renal-cell carcinoma: current status and future perspectives. *Lancet Oncol* 2007; **8**: 554–8.
22 Novara G, Ficarra V, Antonelli A *et al.* Validation of the 2009 TNM version in a large multi-institutional cohort of patients treated for renal cell carcinoma: are further improvements needed? *Eur Urol* 2010; **58**: 588–95.
23 ggener S. TNM staging for renal cell carcinoma: time for a new method. *Eur Urol* 2010; **58**: 517–9; discussion 9–21.
24 Patard JJ, Kim HL, Lam JS *et al.* Use of the University of California Los Angeles integrated staging system to predict survival in renal cell carcinoma: an international multicenter study. *J Clin Oncol* 2004; **22**: 3316–22.
25 Thompson RH, Leibovich BC, Lohse CM *et al.* Dynamic outcome prediction in patients with clear cell renal cell carcinoma treated with radical nephrectomy: the D-SSIGN score. *J Urol* 2007; **177**: 477–80.
26 Iimura Y, Saito K, Fujii Y *et al.* Development and external validation of a new outcome prediction model for patients with clear cell renal cell carcinoma treated with nephrectomy based on preoperative serum C-reactive protein and TNM classification: the TNM-C score. *J Urol* 2009; **181**: 1004–12; discussion 12.
27 McCormick RI, Blick C, Ragoussis J *et al.* miR-210 is a target of hypoxia-inducible factors 1 and 2 in renal cancer, regulates ISCU and correlates with good prognosis. *Br J Cancer* 2013; **108**: 1133–42.
28 Huang L, Luo J, Cai Q *et al.* MicroRNA-125b suppresses the development of bladder cancer by targeting E2F3. *Int J Cancer* 2011; **128**: 1758–69.
29 Shi XB, Xue L, Ma AH, Tepper CG, Kung HJ, White RW. miR-125b promotes growth of prostate cancer xenograft tumor through targeting pro-apoptotic genes. *Prostate* 2011; **71**: 538–49.
30 Gong J, Zhang JP, Li B *et al.* MicroRNA-125b promotes apoptosis by regulating the expression of Mcl-1, Bcl-w and IL-6R. *Oncogene* 2013; **32**: 3071–9.
31 Guan Y, Yao H, Zheng Z, Qiu G, Sun K. MiR-125b targets BCL3 and suppresses ovarian cancer proliferation. *Int J Cancer* 2011; **128**: 2274–83.
32 Hofmann MH, Heinrich J, Radziwill G, Moelling K. A short hairpin DNA analogous to miR-125b inhibits C-Raf expression, proliferation, and survival of breast cancer cells. *Mol Cancer Res* 2009; **7**: 1635–44.
33 Bousquet M, Quelen C, Rosati R *et al.* Myeloid cell differentiation arrest by miR-125b-1 in myelodysplastic syndrome and acute myeloid leukemia with the t(2;11)(p21;q23) translocation. *J Exp Med* 2008; **205**: 2499–506.
34 Xia HF, He TZ, Liu CM *et al.* MiR-125b expression affects the proliferation and apoptosis of human glioma cells by targeting Bmf. *Cell Physiol Biochem* 2009; **23**: 347–58.
35 Nishida N, Yokobori T, Mimori K *et al.* MicroRNA miR-125b is a prognostic marker in human colorectal cancer. *Int J Oncol* 2011; **38**: 1437–43.
36 Medrano S, Monteagudo MC, Sequeira-Lopez ML, Pentz ES, Gomez RA. Two microRNAs, miR-330 and miR-125b-5p, mark the juxtaglomerular cell

and balance its smooth muscle phenotype. *Am J Physiol Renal Physiol* 2012; **302**: F29–37.
37 Ferracin M, Bassi C, Pedriali M *et al.* miR-125b targets erythropoietin and its receptor and their expression correlates with metastatic potential and ERBB2/HER2 expression. *Mol Cancer* 2013; **12**: 130.
38 Wan Y, Fei XF, Wang ZM *et al.* Expression of miR-125b in the new, highly invasive glioma stem cell and progenitor cell line SU3. *Chin J Cancer* 2012; **31**: 207–14.
39 von Brandenstein M, Pandarakalam JJ, Kroon L *et al.* MicroRNA 15a, inversely correlated to PKCalpha, is a potential marker to differentiate between benign and malignant renal tumors in biopsy and urine samples. *Am J Pathol* 2012; **180**: 1787–97.
40 Fritz HK, Lindgren D, Ljungberg B, Axelson H, Dahlback B. The miR(21/10b) ratio as a prognostic marker in clear cell renal cell carcinoma. *Eur J Cancer* 2014; **50**: 1758–65.
41 Haemmig S, Baumgartner U, Gluck A *et al.* miR-125b controls apoptosis and temozolomide resistance by targeting TNFAIP3 and NKIRAS2 in glioblastomas. *Cell Death Dis* 2014; **5**: e1279.
42 Gurova KV, Hill JE, Guo C *et al.* Small molecules that reactivate p53 in renal cell carcinoma reveal a NF-kappaB-dependent mechanism of p53 suppression in tumors. *Proc Natl Acad Sci U S A* 2005; **102**: 17448–53.
43 Parlato S, Bruni R, Fragapane P *et al.* IFN-alpha regulates Blimp-1 expression via miR-23a and miR-125b in both monocytes-derived DC and pDC. *PLoS ONE* 2013; **8**: e72833.
44 Wang YD, Cai N, Wu XL, Cao HZ, Xie LL, Zheng PS. OCT4 promotes tumorigenesis and inhibits apoptosis of cervical cancer cells by miR-125b/BAK1 pathway. *Cell Death Dis* 2013; **4**: e760.
45 Gazda LS, Martis PC, Laramore MA *et al.* Treatment of agarose-agarose RENCA macrobeads with docetaxel selects for OCT4(+) cells with tumor-initiating capability. *Cancer Biol Ther* 2013; **14**: 1147–57.

Supporting Information

Additional supporting information may be found in the online version of this article:

Fig. S1. Expression of miR-125b in sections of clear-cell renal carcinoma.

Table S1. Relation between miR-125b expression and clinical characteristics in the training and validation sets.